Proceedings of the 28th IEEE
EMBS Annual International Conference
New York City, USA, Aug 30-Sept 3, 2006

Fast Oscillatory Rhythms In Inspiratory Motor Discharge: A Mathematical Model

Xinnian Chen, Irene C. Solomon, He Zhao and Ki H. Chon, *Member, IEEE*

***Abstract*—in this paper, a mathematic model is applied to characterize spectral activity associated with fast oscillatory rhythms inherent in inspiratory discharges. Based on the estimated parameters, features are extracted to allow the model to discriminate between changes in the location, magnitude, and shape of spectral activities under basal conditions and during pharmacological blockade of gap junctions.**

I. Introduction

FAST oscillatory neuronal activity, which may serve as an index for synchronization of neuronal discharges, is a prominent feature observed in many CNS areas, including regions associated with motor control. In the respiratory neural control system, it has long been recognized that, in addition to a slow rhythm associated long-time scale features of respiratory cycle timing (*i.e.*, respiratory frequency), fast oscillatory rhythms, associated with short-time scale neuronal synchrony, are presented in inspiratory-related muscles, nerves, and neurons. Power spectral density (PSD) of phrenic nerve discharge has provided insight into the frequency components of fast oscillatory rhythms within the inspiratory phase. Two dominant peaks in the power spectrum, referred to as medium (MFO) and high frequency oscillations (HFO) [1,2], have been identified in all adult mammalian species studied thus far, and these two peaks provide an index of inspiratory-phase neuronal synchronization. Changes in spectral power and/or peak frequencies underlying these fast oscillatory rhythms can be modified by different physiological and pathological states (*e.g.*, hypercapnia, hypoxia, maturation, temperature) as well as in response to pharmacological manipulations of the brainstem respiratory neural network (*e.g.*, activation or blockade of receptors/channels). Previous work from our laboratory, for example, has demonstrated that pharmacological blockade of gap junction coupling in an arterially-perfused adult rat preparation elicits not only a decrease in amplitude and an increase in frequency of phrenic bursts but also a reduction in spectral power in both the MFO and HFO ranges, suggesting reconfiguration of the central inspiratory neural network [3]. Although general features (*e.g.*, peak frequencies or power) could be extracted from the frequency output, systematic interpretations about the power spectrum are still necessary and missing. Knudsen and colleagues have developed a mathematical model to track the frequency changes in renal blood flow between normal-tension and hyper-tension rats, and this model has successfully allowed for differentiation between these two conditions [4]. To gain a better understanding of the spectral dynamics underlying inspiratory motor discharge and its modulation by gap junction blockade, we applied this type of mathematical modeling approach to fit the major dynamic features (*i.e.*, frequency content) of the inspiratory burst. In order to represent the dynamic features of MFO and HFO, the model contained 9 parameters, which were optimized to fit the PSD characteristics both before and after blockade of gap junctions by applying a nonlinear least squares method. This approach allowed for quantification of the dominant spectral peaks and power distribution (*i.e.*, shape) as well as the ability to differentially discriminate between changes in MFO and HFO spectral activities. The results of the model were then compared to the experimental data obtained from 6 arterially-perfused adult rat preparations under baseline conditions and during blockade of gap junctions by perfusion with the gap junction blocker carbenoxolone (CBX; 100 μM final concentration).

II. Mathematical Model

To quantify the characteristics associated with the dominant peaks represented in the PSD of each phrenic burst, a second order system was applied (Eq. 1), with the location of the peak being determined by the primary frequency ω_0 and the shape of the peak resulting primarily from the damping coefficient d.

Assuming the MFO and HFO are generated and modified by two components in the central respiratory control network that are connected in series, as suggested by the literature [1], the overall frequency representation of an inspiratory burst can be suggested by multiplication of the two second-order systems by the overall system gain k, as shown in Eq. (2).

Manuscript received May 13, 2006. This work was supported by the National Institutes of Health under Grants NS045321 and NS049310.

X. Chen is with the Department of Biomedical Engineering, Stony Brook University, Stony Brook, NY 11794 USA. (Phone: 631-444-2354; fax: 631-444-3432; e-mail: xinnchen@ic.sunysb.edu).

I. C. Solomon is with the Department of Physiology and Biophysics, Stony Brook University, Stony Brook, NY 11794 USA. (E-mail: Irene.Solomon@sunysb.edu).

H. Zhao is with the Department of Biomedical Engineering, Stony Brook University, Stony Brook, NY 11794 USA. (E-mail: hezhao@ic.sunysb.edu)

K. H. Chon is with the Biomedical Engineering Department, Stony Brook University, Stony Brook, NY 11794 USA. (E-mail: Ki.Chon@sunysb.edu).

$$H(s) = \frac{\frac{s^2}{\omega'^2_0} + \frac{2d's}{\omega'_0} + 1}{\frac{s^2}{\omega_0^2} + \frac{2d's}{\omega_0} + 1} \quad (1)$$

$$H(\omega) = K \cdot \frac{\frac{\omega^2}{\omega'^2_{MFO}} + \frac{2d'_{MFO}\,\omega}{\omega'_{MFO}} + 1}{\frac{\omega^2}{\omega_{MFO}^2} + \frac{2d_{MFO}\omega}{\omega_{MFO}} + 1} \cdot \frac{\frac{\omega^2}{\omega'^2_{HFO}} + \frac{2d'_{HFO}\,\omega}{\omega'_{HFO}} + 1}{\frac{\omega^2}{\omega_{HFO}^2} + \frac{2d_{HFO}\omega}{\omega_{HFO}} + 1} \quad (2)$$

$$\theta = (\mathrm{K}\ \omega'_{\mathrm{MFO}}\ \ d'_{\mathrm{MFO}}\ \ \omega_{\mathrm{MFO}}\ d_{\mathrm{MFO}}\ \omega'_{\mathrm{HFO}}\ d'_{\mathrm{HFO}}\ \ \omega_{\mathrm{HFO}}\ d_{\mathrm{HFO}})$$

Thus, to represent the frequency content using the above model, 9 parameters were assigned, as vector θ. Fig. 1 shows an example of the spectral peaks generated using Eq. (2). Note that combination of the left and right side of Eq. (2) is responsible for the generation of the two spectral peaks shown in Fig. 1.

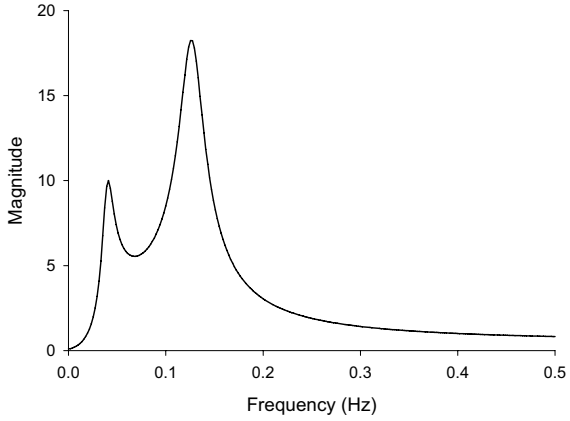

Fig. 1. Example of two resonance peaks generated using the 9 parameter mathematic model.

The model also reflects the transformed Laplace transfer function of the central neural network that generates inspiratory motor output, represented by Eq. (3), which reflects a black box with a random signal as the input to the central controller and the output is inspiratory motor discharge.

$$H(s) = K \cdot \frac{\frac{s^2}{\omega'^2_{MFO}} + \frac{2d'_{MFO}\,s}{\omega'_{MFO}} + 1}{\frac{s^2}{\omega_{MFO}^2} + \frac{2d_{MFO}s}{\omega_{MFO}} + 1} \cdot \frac{\frac{s^2}{\omega'^2_{HFO}} + \frac{2d'_{HFO}\,s}{\omega'_{HFO}} + 1}{\frac{s^2}{\omega_{HFO}^2} + \frac{2d_{HFO}s}{\omega_{HFO}} + 1} \quad (3)$$

The model parameters are optimized using a nonlinear least squares method. To start the optimization, initial parameter values were assigned based on values from previous studies [1,2,3]. For optimization of ω_{MFO} and ω_{HFO}, initial values were set to 50 Hz and 100 Hz, respectively, and were restricted within a range of MFO and HFO values previously defined. Since there is no *a priori* information about the other model parameters, no restrictions were set for these.

III. RESULTS

A. Simulation Results

Data were generated for two simulations using Matlab 6.5. In both simulations, two main peaks were generated, with one peak located at 38 Hz and the other at 120 Hz. In the second simulation, however, the shape and power distribution of the PSD was modified in order to further assess the capabilities (*i.e.*, adequacy and accuracy) of the 9 parameter model. Fig. 2 shows the PSD and model fitting results from these two simulations. In each plot, the solid black line corresponds to the PSD results of the simulation and the dotted red line represents the results of the mathematical model.

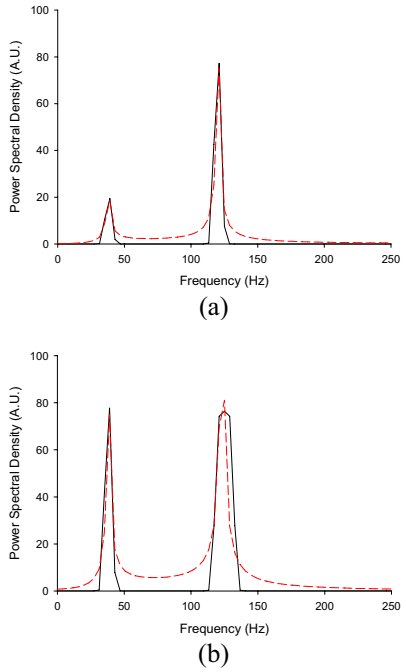

Fig. 2. Examples comparing the PSD results from simulation data with the performance of the 9 parameter mathematical model. In both cases, two resonance peaks were generated, but each simulation had a different power ratio and power distribution.

The results from the above simulations demonstrate that the 9 parameter model is capable of adequately and accurately identifying the frequencies, magnitudes, and shapes of the peaks as determined by the PSD analysis. It should be noted, however, that the spectral peaks determined by the PSD analysis method were based on 256 parameters while those of the mathematical model were based on only 9 parameters, demonstrating that the 9 parameter model greatly increases the efficiency of spectral representation. These realizations

reflect differences in the parameter values (*i.e.*, system gain, damping coefficients, etc.) obtained for each simulation. Thus, in simulation 2 (as compared to simulation 1), the increase in power of the low frequency (38 Hz) peak corresponds to an increase in the system gain, which is reflected by an increase in the value of k, and the change in the shape and power distribution of both the low (38 Hz) and high (120 Hz) frequency peaks correspond to a reduction in the damping coefficient, which is reflected by a decrease in d_{MFO} and d_{HFO}, respectively.

B. Experimental Results

The experimental data used for this study correspond to a series of experiments previously conducted using an *in vitro* arterially-perfused decerebrate adult rat (81-125g, ~5-6 wk old; n = 6) preparation [3]. In these experiments, phrenic nerve activity was recorded under baseline conditions and during blockade of gap junctions by perfusion with the gap junction blocker carbenoxolone (CBX; 100 µM final concentration). Phrenic nerve discharge was amplified (x10k), notch filtered (60Hz), analog filtered to pass frequencies between 10Hz and 1kHz, and recorded simultaneously on a computer at a sampling rate of 2 kHz (Chart 5.0, PowerLab, ADInstruments) and on a DAT recorded at a sampling rate of 2.5 kHz (C-DAT16, Cygnus Technology Inc.) for off-line analyses (MatLab 6.5).

For these analyses, 5-minute traces of phrenic nerve discharge under baseline conditions and during perfusion with CBX were extracted from the time series trace. These data were the segmented to obtain to data lengths corresponding to the inspiratory bursts (with little or no post-inspiratory discharge). These phrenic burst data were re-sampled with a sampling rate of 500 Hz, after digital band-pass filtering (20-250 Hz, using a 6th order Butterworth filter). Each data burst was demeaned and normalized to allow for direct comparisons of spectral composition between conditions. For computation of PSD, Welch's periodogram method was used. PSD data are reported as an ensemble average derived from analyses of 10 phrenic bursts under each condition.

Fig. 3 provides an example of phrenic nerve discharge, and its corresponding PSD, before and during blockade of gap junctions using CBX. Panel (A) shows 30-second traces of raw and integrated phrenic nerve discharge under baseline (control) conditions and at ~10 minutes of perfusion with CBX and panel (B) shows the ensemble-averaged PSD data (solid black line) corresponding to these time points. As can be seen, perfusion with CBX modifies the amplitude and frequency of phrenic bursts as well as the PSD. For the 6 experiments conducted, the amplitude of integrated phrenic nerve discharge was reduced by ~50% of baseline (control) and the frequency of phrenic bursts approximately doubled during perfusion with CBX. In addition, the power of the HFO peak was markedly reduced during perfusion with CBX.

C. Using Mathematical Model on Experimental Data

Also shown in Fig. 3 (B) are the results obtained from fitting the mathematical model to these experimental data. In these plots, the model results (dotted red line) for each experimental condition are overlaid on the PSD results of the experimental data (solid black line). As can be seen, the 9 parameter mathematical model accurately predicted the amplitude, shape, and frequencies of dominant spectral activities (a) under baseline conditions as well as (b) during perfusion with CBX. Thus, the model was able to track the primary changes in spectral activity observed during blockade of gap junctions.

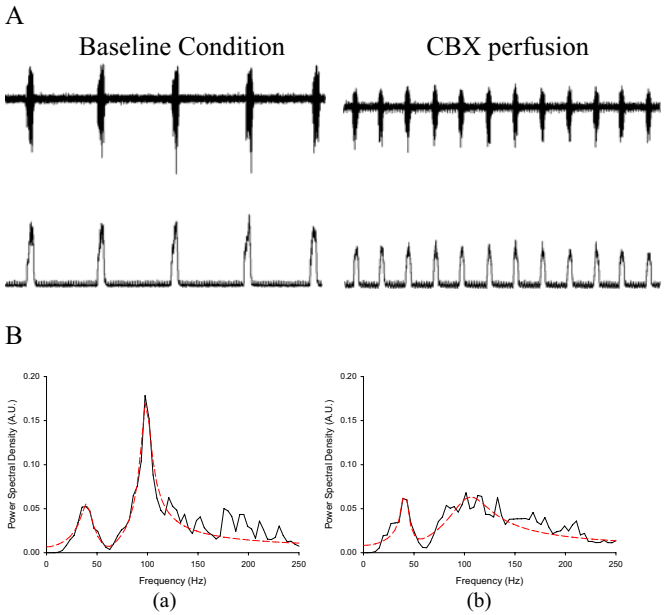

Fig. 3. Examples demonstrating modulation of phrenic nerve discharge by pharmacological blockade of gap junctions using CBX. A: Raw and integrated phrenic nerve discharge. During perfusion with CBX, phrenic burst amplitude was reduced and phrenic burst frequency was increased. B: Results from PSD analysis and fitting the mathematical model under (a) baseline conditions and (b) during perfusion with CBX. During perfusion with CBX, HFO power was markedly reduced. Note that the marhematical model accurately fit the experimental data under both conditions. PSD, solid black line; mathematical model, dotted red line.

The model parameter values corresponding to baseline conditions and perfusion with CBX are provided in Table 1. These values correspond to 10 burst ensemble-averages for each minute of a 5-minute recording for each of the 6 experiments conducted. The most notable changes observed in the model parameter values are associated with HFO activity during perfusion in CBX. For example, the damping coefficient of the HFO d_{HFO} was decreased ($P<0.05$), which corresponds to the alteration in the shape and the decrease in amplitude of HFO activity observed in model fit as well as the experimental data. In addition, the model identified a reduction of system gain k during CBX perfusion, suggesting a global reduction in the power associated with the fast oscillatory rhythms, which presumably also reflects the effects seen on HFO power. In contrast to the experimental

data, the mathematical model identified an upward shift in the resonance frequency of the HFO peak ω_{HFO} during CBX perfusion; this difference, however, may be due to the marked reduction (*i.e.*, loss) of a distinct HFO peak in the experimental data in some experiments. Finally, no significant changes in the model parameter values were noted for MFO activity, which most likely reflects the fact that the experimental data and the fitted model show little or no effect on the shape and amplitude of MFO activity.

TABLE I
MODEL PARAMETER VALUES
FOR BASELINE AND CBX PERFUSION CONDITIONS

Parameter	Baseline	CBX Perfusion
k	0.0043±0.0004	0.0015±0.0005*
ω_{MFO}	44.26±2.97	34.8±0.42
d_{MFO}	0.199±0.038	0.180±0.027
ω'_{MFO}	146.12±22.33	413.40±202.88
d'_{MFO}	4.392±0.922	2.440±0.646
ω_{HFO}	98.94±6.32	121.32±7.67*
d_{HFO}	0.148±0.044	0.252±0.043*
ω'_{HFO}	0.353±0.036	0.240±0.020*
d'_{HFO}	0.221±0.112	0.806±0.259

Mean ± standard error for identified model parameter values under baseline and CBX perfusion conditions.
*Indicates a statistically significant difference ($p<0.05$) between baseline and CBX perfusion based on paired t-test.

IV. CONCLUSION

Numerous studies in respiratory neural control have implemented PSD methods to identify and characterize frequency content of inspiratory-related bursts. These studies have provided data pertaining to the relative power, area, and/or location of dominant spectral peaks; however, there are many instances when it would be valuable to better quantify the strength and further characterize the dynamics of MFO and HFO activities, including the shape and power distribution. In this study, we applied a 9 parameter mathematical model to both simulation and experimental data, and demonstrated that the model is able to adequately and accurately track induced changes in spectral activity. For example, the implemented model was able to predict the amplitude, shape, and frequencies of dominant spectral activities under baseline conditions and during modulation of HFO activity elicited by blockade of gap junctions. Further, the model was able to identify that no modulation of MFO activity occurred during blockade of gap junctions. This differential discrimination of the effects on MFO versus HFO suggests that the mathematical model may enhance our ability to identify and quantify the mechanisms that may contribute to the generation of MFO and/or HFO activities. We suggest that the proposed mathematical model provides a promising tool for further examination of spectral dynamics in inspiratory motor discharge, including their modulation under various pathological states and during pharmacological perturbations.

ACKNOWLEDGMENT

The authors thank Melissa N. Rodriguez for contribution of the experimental data used in this study.

REFERENCES

[1] M.I. Cohen, W.R. See, C.N. Christakos, A.L. Sica. "High-frequency and Medium-frequency Components of Different Inspiratory Nerve Discharges and their Modification by Various Inputs" *Brain Res* 417: 148-152, 1987.

[2] C.A. Richardson, R.A. Mitchell. "Power Spectral Analysis of Inspiratory Nerve Activity in the Decerebrate Cat" *Brain Res* 233: 317-336,1982.

[3] I.C. Solomon, K.H. Chon, M.N. Rodriguez. "Blockade of Brain Stem Gap Junctions Increases Phrenic Bursts Frequency and Reduces Phrenic Burst Synchronization in Adult Rat" *J Neurophysiol*, 89: pp. 135-149 2003.

[4] T. Knudsen, H. Elmer, M. Knudsen, N.H. Holstein-Rathlou, J. Stoustrup. "Dynamic Modeling of Renal Blood Flow in Dahl Hypertensive and Normotensive Rats" *IEEE Transactions on Biomeical Engineering,* vol. 51, No. 5, May 2004.